Published in final edited form as:
J Immunol. 2013 September 15; 191(6): 2871–2878. doi:10.4049/jimmunol.1202323.

The tetraspanin CD63 is required for efficient IgE-mediated mast cell degranulation and anaphylaxis1

Stefan Kraft[1,4], **Marie-Hélène Jouvin**[1], **Nitin Kulkarni**[1], **Sandra Kissing**[2], **Ellen S. Morgan**[3], **Ann M. Dvorak**[3], **Bernd Schröder**[2], **Paul Saftig**[2,*], and **Jean-Pierre Kinet**[1,*]

[1]Laboratory of Allergy and Immunology, Department of Pathology, Beth Israel Deaconess Medical Center, Boston, MA, USA

[2]Institute of Biochemistry, University of Kiel, Germany

[3]Center for Vascular Biology Research, Beth Israel Deaconess Medical Center, Boston, MA, USA

[4]Department of Pathology, Massachusetts General Hospital, Boston, MA, USA

Abstract

Mast cell activation through the high affinity IgE receptor FcεRI leads to the release of mediators involved in immediate-type allergic reactions. While antibodies against the tetraspanins CD63 and CD81 inhibit FcεRI-induced mast cell degranulation, the intrinsic role of these molecules in FcεRI-induced mast cell activation is unknown. In mast cells, CD63 is expressed at the cell surface and in lysosomes (particularly secretory lysosomes that contain allergic mediators). Here, we investigated the role of CD63 in mast cells using a CD63 knockout mouse model. CD63-deficiency did not affect *in vivo* mast cell numbers and tissue distribution. Bone-marrow-derived mast cells (BMMC) developed normally in the absence of CD63 protein. However, CD63-deficient BMMC showed a significant decrease in FcεRI-mediated degranulation, but not PMA/ionomycin-induced degranulation, as shown by β-hexosaminidase release assays. The secretion of TNF-α, which is both released from granules and synthesized *de novo* upon mast cell activation, was also decreased. IL-6 secretion, and production of the lipid mediator leukotriene C4 were unaffected. There were no ultrastructural differences in granule content and morphology, late endosomal/lysosomal marker expression, FcεRI-induced global tyrosine phosphorylation, and Akt phosphorylation. Finally, local reconstitution in genetically mast cell-deficient $Kit^{w/w\text{-}v}$ mice was unaffected by the absence of CD63. However, the sites reconstituted with CD63-deficient mast cells developed significantly attenuated cutaneous anaphylactic reactions. These findings demonstrate that the absence of CD63 results in a significant decrease of mast cell degranulation, which translates into a reduction of acute allergic reactions *in vivo*, thus identifying CD63 as an important component of allergic inflammation.

INTRODUCTION

Mast cells (MC) originate in the bone marrow and migrate to most connective tissues and mucosa/epithelia in processes that involve various integrins and extracellular matrix proteins (1). Within those peripheral tissues, MC mature and can be long-lived, constitutional tissue

[1]This work was supported by a NIH grant (RO1 AI41087) to JPK and grants from the Deutsche Forschungsgemeinschaft (DFG-GRK1459; SPP1480) and the Center of Excellence Inflammation at Interfaces to P.S and B.S.

[*]Corresponding Authors: Jean-Pierre Kinet, Laboratory of Allergy and Immunology, Department of Pathology, Beth Israel Deaconess Medical Center, 99 Brookline Ave, Boston, MA 02215, USA, kinet@bidmc.harvard.edu, Tel.: +1-617-667-2816, Fax: +1-617-667-1323, Paul Saftig, University Kiel, Biochemical Institute, Otto-Hahn Platz 9, 24098 Kiel, Germany, psaftig@biochem.uni-kiel.de, Tel: +49-431-8802216, Fax: +49-431-8802238.

residents, or recruited to sites of inflammation. Their best established role is in IgE-mediated allergic reactions, but they also positively and negatively regulate multiple aspects of the inflammatory reaction in autoimmunity, contact hypersensitivity, cancer response, and host defense directly and indirectly by influencing dendritic cells, Th1, Th2, Treg and Th17 cells, endothelial cells, neurons, and possibly B cells (2, 3). These effects are mediated by the numerous mediators that MC release upon activation. Two main release mechanisms operate in MC. Mediators such as histamine, serotonin, proteases, IL-4, and also a significant proportion of TNF-α, are preformed and stored in granules from which they are released upon MC activation in a process called degranulation or regulated exocytosis. Others, such as numerous cytokines, leukotrienes, and prostaglandins are synthesized *de novo* and released upon MC activation (4–8).

MC can be activated by various mechanisms, such as immunoglobulins, cytokines, physical factors, and microbial products. MC activation takes place in acute IgE-mediated allergic reactions such as anaphylaxis. In this case, antigen-specific IgE bound to its high affinity receptor FcεRI expressed at the surface of MC is crosslinked by multivalent antigens, leading to the activation of multiple signaling cascades. Key features are the activation of protein tyrosine kinases of the src and syk family, multiple downstream adapter molecules, GTPases, and serine-threonine kinases, and calcium mobilization, which ultimately results in the release of the different mediators (7, 9, 10).

FcεRI-induced MC activation can be positively or negatively affected by a variety of mechanisms (11). One involves tetraspanins, proteins that are expressed in various membrane compartments and regulate cell morphology, motility, invasion, fusion and signaling (12–14). Using monoclonal antibodies (mAb) that recognize antigens expressed at the surface of MC and inhibit FcεRI-induced mast cell degranulation, we previously identified the tetraspanins CD63 and CD81 as regulators of FcεRI-induced mast cell activation (15, 16). Anti-CD63 inhibits MC degranulation without affecting early signals, such as protein tyrosine phosphorylation and calcium mobilization, suggesting that it interferes with exocytosis (16). CD63 is known to be expressed in intracellular membranes, such as secretory lysosomes including serotonin-containing granules (17–20). Upon basophil degranulation, CD63 expression at the plasma membrane increases, and is classically used as a marker of basophil activation (21). Recently, an isoform of CD63 has been identified as specific form of CD63 expressed at the plasma membrane in degranulated MC (22). Anti-CD63 also inhibits adhesion of the MC model cell line RBL-2H3 to extracellular matrix proteins, which could be explained by the known interaction of CD63 with integrins in plasma membrane microdomains, or by inhibition of signaling mechanisms common to FcεRI and integrins (16, 23, 24).

Recently, CD63-deficient mice were generated. In spite of the broad tissue and cell distribution of CD63, these mice display no obvious morphologic or functional abnormalities of their lysosomes (25). However, they exhibit morphologic changes in the collecting ducts in the kidneys, a disturbed water balance (25), defective endosomal protein sorting during melanogenesis (26), and leukocyte recruitment (27).

To further investigate the role of CD63 in MC *in vivo*, we took advantage of the availability of these CD63-deficient mice.

MATERIALS AND METHODS

Mice and bone marrow-derived mast cells (BMMC)

The generation and characterization of CD63-deficient mice were described previously (25). MC-deficient $Kit^{w/w\text{-}v}$ mice were obtained from Jackson Labs (Bar Harbor, ME). Mice were

housed in a pathogen-free barrier facility at the Center for Life Sciences, Boston, MA. Studies were conducted in accordance with the National Institutes of Health *Guide for the Care and Use of Laboratory Animals* as well as the Institutional Animal Care and Use Committee (IACUC) guidelines of the Animal Research Facility at Beth Israel Deaconess Medical Center. BMMC were generated from 4 to 8 week-old mice by isolating bone marrows and tibias. Cells were then cultured in IMDM (Corning Cellgro, Mediatech Inc., Manassas, VA) supplemented with 10% fetal bovine serum, nonessential amino acids (Corning Cellgro), 50 μM β-mercaptoethanol (Sigma Aldrich, St. Louis, MO), and 3 ng/ml IL-3 (Peprotech, Rocky Hill, NJ). After 4 weeks of culture, purity of BMMC cultures was assessed by morphology and flow cytometric analysis of c-Kit expression using a FITC-conjugated anti c-Kit monoclonal antibody (BD Biosciences, San Jose, CA). FcεRI expression was determined by labeling with IgE (Sigma Aldrich) and an anti-IgE FITC conjugated antibody (BD Biosciences). Sections from different organs were subject to formalin fixation, and paraffin embedding in a routine histopathologic laboratory according to standard procedures. Sections were stained with 0.1 % toluidine blue solution (Sigma).

Electron microscopy and Giemsa staining of BMMC

For electron microscopy, the BMMC were fixed in a dilute mixture of aldehydes, washed in 0.1 M sodium cacodylate buffer, and spun through molten agar to form agar blocks containing the cells. The blocks were processed for electron microscopic studies as described using a Philips CM10 electron microscope (28). In addition, Giemsa stains were performed on 1 μm sections from agar blocks and analyzed by light microscopy.

Indirect immunofluorescence and confocal microscopy analysis

Coverslips were coated in 100 μg/ml poly-L-lysine (Sigma-Aldrich) overnight and washed twice with water for 1 h before use. BMMC were fixed in 4% (wt/vol) paraformaldehyde in PBS for 20 min at room temperature. Immunocytochemical stainings were performed as described previously (29) with anti-LAMP1 (1D4B; Developmental Studies Hybridoma Bank, Iowa City, IA), anti-LAMP2 (ABL93; Developmental Studies Hybridoma Bank), anti-cathepsin D (30), anti-CD63 (25), and anti-LIMP-2 (31) as primary antibodies. Alexa Fluor 488– or 594– conjugated goat anti–rat IgG or goat anti–rabbit IgG were used as secondary antibodies (MoBiTec, Göttingen, Germany), respectively. Coverslips were mounted on glass slides in a medium containing 17% Mowiol 4–88 (EMD Millipore, Billerica, MA), 33% glycerol, and 20 mg/ml DABCO (1,4-diaza-bicyclo-[2,2,2]-octane) in PBS. Nuclei were visualized with DAPI (4-,6-diamidino-2-phenylindole; Sigma) added to the embedding medium at a concentration of 1 μg/ml. Photographs of optical sections were acquired with an FV1000 confocal laser scanning microscope (Olympus, Tokyo, Japan) equipped with an U Plan S Apo 100°— oil immersion objective (N.A. 1.40) and Olympus Fluoview Software (3.0a).

Immunoblotting

BMMC were solubilized in lysis buffer (50 mM Tris pH 7.4, 150 mM NaCl, 5 mM EDTA, 1% (vol/vol) Triton X-100), followed by centrifugation and resuspension in SDS sample buffer without β-mercaptoethanol. SDS-PAGE and immunoblotting were performed using 10% polyacrylamide gels. Anti-mouse CD63 rabbit antiserum (25) was used at a 1:400 dilution and control anti-FcεRIβ monoclonal antibody supernatant (JRK1 (32)) pure, followed by incubation with horseradish-peroxidase conjugated anti-rabbit and anti-mouse antibodies (Sigma). Anti-phosphotyrosine (4G10, Millipore, Billerica, MA), anti-phospho-Akt (anti phosphoserine 473 Akt; Cell Signaling Technology, Beverly, MA) and anti-Akt blots (Cell Signaling Technology) of cells triggered as described for degranulation assays were performed as described in (16, 33).

Degranulation Assays

For assessment of MC degranulation, β-hexosaminidase assays were performed. Briefly, 1×10^6/ml BMMC were loaded with 1 μg/ml anti-DNP IgE (Sigma) in culture medium without IL-3 over night. Then, cells were washed 3× in Modified Tyrode's Buffer (135 mM NaCl, 5 mM KCl, 1 mM $MgCl_2$, 10 mM Hepes, 5.6 mM dextrose, 0.1 % (wt/vol) BSA), and then triggered for 30 minutes at 37°C with 0 – 100 ng/ml DNP-BSA (Sigma) or 2 – 10 nM PMA in combination with 0.5 – 2 μM ionomycin, at 4×10^6 cells/ml. After stimulation, cells were centrifuged at 4°C and supernatants were incubated in citrate buffer (50 mM citric acid, 50 mM sodium citrate, pH = 4.5) with 0.3 mg/ml p-nitrophenyl N-acetyl-β-D-glucosaminide (Sigma) for 60 minutes at 37°C. Cell pellets were lysed in a Modified Tyrode's solution with 1% (vol/vol) Triton X-100 and also incubated in citrate buffer. Reactions were terminated in carbonate buffer (100 mM Na_2CO_3, 100 mM $NaHCO_3$), and after 15 minutes OD at 405 nM was determined using an ELISA plate reader. Specific release was calculated as % of total β-hexosaminidase content after subtraction of baseline degranulation in untriggered cells.

LTC4 production

BMMC were loaded and triggered similar to β-hexosaminidase assays except that culture medium for overnight loading contained IL-3 and cell concentration during triggering was 0.5×10^6/ml. After triggering, LTC4 and PGD2 production was determined using an EIA assay (Cayman Chemical, Ann Arbor, MI) according to manufacturer's instructions.

TNF-a and IL-6 ELISA

BMMC were loaded with 0.5 μg/ml anti-DNP IgE over night in culture medium without IL-3. Then cells, were washed and incubated for 6 hours at 0.25×10^6 cells/ml in culture medium with 0–100 ng/ml DNP-BSA. ELISA was performed using kits (BD Biosciences) according to manufacturer's instructions.

Adoptive transfer of BMMC to $Kit^{w/w\text{-}v}$ mice and passive cutaneous anaphylaxis (PCA)

Transfer of CD63+/+ and CD63−/− BMMC into MC-deficient $Kit^{w/w\text{-}v}$ mice (3, 34) was performed by intradermal injection of 1×10^6 BMMC in PBS + 10 μg/ml mouse serum albumin (Sigma) each into ear skin. After 4 weeks, PCA was performed as described previously (34) with some modifications. Briefly, 100 ng anti-DNP IgE (or control buffer) in PBS + 10 μg/ml mouse serum albumin was injected intradermally into ear skin. On the next day, PCA was elicited by injecting 200 μg of DNP-BSA in 0.9 % (wt/vol) NaCl containing 1% (wt/vol) Evan's blue (Sigma) intravenously into tail veins. After 30 minutes, mice were sacrificed and development of anaphylactic reactions was determined by measuring the amount of leaked Evan's Blue extracted in formamide (three incubations for 2 hours each at 60°C) from 5 mm ear skin punches. The average amount of dye extracted from ears of mice that were injected in buffer (without DNP-IgE) was used as a baseline control and was subtracted from test values. Additional mice were subject to PCA, followed by use of ear skin for histopathology and toluidine blue staining. A value of more than 10% of granules released from the mast cell cytoplasm was used to determine the number of degranulated mast cells in tissue sections.

RESULTS

CD63 −/− mice show normal mast cell numbers and tissue distribution

To evaluate the role of CD63 in mast cells (MC), CD63-deficient mice were analyzed in detail (25). Many tetraspanins regulate cell motility in conjunction with integrins (12). Thus, CD63 deletion could affect the migration, homing and maturation of MC from the bone

marrow into tissues (1). To determine whether CD63-deficient mice show any abnormalities in MC development and tissue distribution, paraffin-embedded sections from skin, stomach, tracheobronchial tree, and heart were prepared from CD63+/+ and CD63−/− littermates. The sections were stained with toluidine blue, which leads to metachromatic staining of MC granules, and the numbers of MC's and their locations within these tissues were compared. Figure 1 shows representative views of bronchial tissues (Fig.1A,B) and the result of MC counts in skin, stomach, tracheobronchial tree, and heart from three mice from each genotype (Fig.1C). No differences were found in MC numbers and locations within these tissues, indicating that CD63 is dispensable for normal MC development and tissue distribution.

FcεRI-induced degranulation is significantly diminished in CD63−/− BMMC

To assess the role of CD63 in MC functions, we generated mouse bone marrow-derived mast cells (BMMC) from CD63+/+ and CD63−/− 6–8 week-old littermates by culture in the presence of IL-3. BMMC developed normally within 3–4 weeks of culture, and showed no obvious differences in morphology (see Fig. 2A and B) and c-Kit and FcεRI expression as determined by flow cytometry (data not shown). To confirm CD63 expression in wild-type BMMC and loss of expression in genetically deficient BMMC, western blot analysis was performed, using a recently described polyclonal antibody (25). As seen in Fig. 2C, BMMC lysates from CD63+/+ mice show a 50–60 kD band representing heterogeneously glycosylated CD63, while this band is absent in BMMC lysates from CD63−/− mice. As a control, the same membrane was blotted with an anti-FcεRIβ Ab. The expression of FcεRIβ was in a comparable range in CD63+/+ and CD63−/− BMMC (Fig. 2D).

Once we had verified the absence of gross abnormalities of CD63-deficient MC, we assessed their response to activation by comparing FcεRI-induced degranulation in CD63+/+ and CD63−/− BMMC. Degranulation was measured by the release of β-hexosaminidase after crosslinking of FcεRI-bound anti-DNP-IgE with the multivalent antigen DNP-BSA. Fig. 3A shows that FcεRI-induced mast cell β-hexosaminidase release is significantly decreased in CD63-deficient BMMC compared to wild type littermates ($p < 0.0001$ by ANOVA). PMA and the calcium ionophore ionomycin can induce degranulation irrespective from FcεRI activation due to the direct activation of PKC and calcium influx. Fig. 3B shows that degranulation induced by PMA and ionomycin was unaffected in CD63-deficient BMMC (while FcεRI-induced triggering was still significantly affected in two concomitant experiments performed in duplicate with 7.4 +/− 1.46% β-hexosaminidase release for CD63+/+ BMMC and 0.0 +/− 0.4% β-hexosaminidase release for CD63−/− BMMC; $p = 0.0016$). In addition, total granule content of β-hexosaminidase (arbitrary units measured from lysates plus supernatant at 405 nm wavelength) was calculated from all β-hexosaminidase assays performed, and was found not to be significantly different (1796 +/− 137 for CD63+/+ ($n = 16$), and 1909 +/− 159 for CD63−/− BMMC ($n = 15$); $p=0.59$). Thus, a granule storage defect in CD63−/− BMMC is unlikely. In summary, CD63 expression is required for efficient MC degranulation via IgE and FcεRI in cell-based assays.

CD63-deficient BMMC exhibit decreased TNF–α secretion, while IL-6 secretion and leukotriene C4 synthesis remain intact

The decrease in degranulation observed in CD63−/− BMMCs could be due to a defect in granule functions, resulting from the absence of CD63 in granules. As opposed to preformed mediators stored in granules, such as histamine, serotonin, and hexosaminidase, other MC mediators such as leukotrienes are synthesized *de novo* (3). Given the role of CD63 in granules/lysosomes, we hypothesized that CD63-deficiency would not affect the release of *de novo* synthesized mediators. To test this hypothesis, we measured FcεRI-induced

leukotriene C4 (LTC4) release in BMMC. As shown in Fig. 4, FcεRI aggregation-induced release of LTC4 is not reduced in CD63-deficient BMMC.

While cytokines such as IL-6 are mostly synthesized upon activation, TNF-α is both synthesized *de novo* and stored within MC for rapid release through regulated exocytosis during degranulation (4–6, 8). We hypothesized that TNF-α release upon FcεRI aggregation would be decreased, while IL-6 release would not be affected by CD63-deficiency. As shown in Fig. 5, the absence of CD63 led to impaired TNF-α secretion (Fig. 5 A), while IL-6 secretion (Fig. 5B) was unaffected.

CD63-deficient BMMC show no ultrastructural abnormalities, differences in lysosomal marker expression, and FcεRI-induced tyrosine and Akt phosphorylation

As shown in Fig. 2 A and B, CD63-deficient BMMC showed no overt light microscopic differences on Giemsa stains. To further investigate possible differences in granule content and morphology, electron microscopic studies were performed (see Fig. 6A and B). Analysis of both CD63+/+ and CD63−/− BMMC showed immature mast cells without discernible ultrastructural differences (two independent experiments performed with n=3 CD63+/+ and n=2 CD63−/− BMMC cultures). In addition, indirect immunofluorescence for the late endosomal/lysosomal marker proteins LIMP-2, LAMP-1, LAMP-2, and cathepsin D and confocal microscopy was performed and showed no obvious differences in expression or distribution of these markers, while CD63 expression was lost in CD63-deficient BMMC (see Figs. 6C–E). Finally, we evaluated proximal FcεRI signaling events. Similar to our prior study using anti-CD63 mediated inhibition of degranulation in RBL (16), global FcεRI-induced tyrosine phosphorylation was unaffected in CD63-deficient BMMC (see supplemental Fig. 1A). However, the Gab2/Akt pathway for degranulation does not appear to be affected in CD63−/− BMMC, as shown by retained Akt phosphorylation (see supplemental Fig. 1B and C).

CD63 contributes significantly to IgE-mediated anaphylactic reactions in vivo

To address the role of CD63 in MC-mediated allergic responses *in vivo*, we took advantage of the congenitally MC-deficient mouse strain $Kit^{W/W\text{-}V}$. These mice can be reconstituted with MC of various genotypes. This model of “mast cell knockin” mice allows for selective analysis of MC-specific functions of genes of interest *in vivo* (3). MC-deficient $Kit^{W/W\text{-}V}$ mice were reconstituted intradermally in one ear with CD63−/− BMMC and in the other ear with the same number of CD63+/+ BMMC. We verified that equal numbers of CD63+/+ and CD63−/− mast cells were present in each ear after reconstitution (Fig. 7A–C).

We then used an established model of IgE- and FcεRI-mediated anaphylaxis, passive cutaneous anaphylaxis, adapted for use in locally reconstituted $Kit^{W/W\text{-}V}$ mice (34). Anaphylaxis was induced by injecting DNP-specific IgE in ears reconstituted with either CD63+/+ or CD63−/− BMMC, followed by triggering with DNP-BSA injected intravenously along with Evan’s blue. Evan’s blue binds to albumin and stays in the vascular system unless it leaks into the tissues when vascular permeability is increased, such as in the case of an acute allergic reaction. The amount of Evan’s blue that can be extracted from ear tissues allows for quantification of the extent of MC degranulation in that ear. In ears reconstituted with CD63−/− BMMC, less Evan’s Blue dye extravasation was observed than in contralateral ears reconstituted with CD63+/+ BMMC (Fig. 7D). For each experiment, the ratio between the amount of Evan’s blue extracted from the CD63−/− ear and the CD63+/+ ear was calculated. The average of this ratio in 7 experiments was 0.49 (SD 0.16; confidence interval 0.34–0.64), which was significantly different from 1 ($p = 0.0002$; t-test). In addition, tissue sections of reconstituted ears prepared after induction of anaphylaxis in a separate experiment performed without Evan’s blue were analyzed. These showed more pronounced

MC in the ear reconstituted with CD63+/+ BMMC, as can be seen by the presence of numerous toluidine blue positive granules outside the MC cytoplasm (Fig. 7 E). The majority of CD63−/− BMMC showed no prominent degranulation (Fig. 7 F). Additional scoring showed that a mean of 71.01% of CD63+/+ BMMC and 26.19% CD63−/− BMMC were degranulated (n=2 slides each).

DISCUSSION

In this study, we showed that the tetraspanin CD63 is required for optimal IgE-mediated MC degranulation and anaphylaxis. Activation of CD63−/− MC generated *ex vivo* led to a significantly decreased secretion of β-hexosaminidase and TNF-α, while production of IL-6 and LTC4 was unaffected. No obvious ultrastructural differences, differences in late endosomal/lysosomal marker expression, as well as alterations in FcεRI-dependent tyrosine phosphorylation were seen in CD63−/− BMMC. However, MC-deficient mice developed significantly less severe passive cutaneous anaphylaxis at sites reconstituted with CD63−/− BMMC compared to sites reconstituted with CD63+/+ BMMC. These strong effects of CD63-deficiency on MC functions are unusual, since knockout models on other tetraspanins often have fallen short of confirming the strong functional effects of antibodies, possibly due to redundant roles in multi-molecular complexes (35).

The discrepancy between the decrease in TNF-α secretion and the preservation of IL-6 and LTC4 production is most likely due their different processing in MC. TNF-α, like mediators such as serotonin, histamine and β-hexosaminidase, is stored in granules and released upon activation by regulated exocytosis (8). A smaller amount of TNF-α is synthesized upon activation and released immediately (4, 6). In MC, CD63 is expressed in secretory lysosomes (SL), structures that possess characteristics of both lysosomes and granules (36). SL are the main organelle responsible for degranulation in nonprofessional secretory cells, such as MC (19, 37–39). CD63 colocalizes with serotonin in RBL cells, a mast cell model cell line (20). SL in RBL cells are capable of regulated secretion upon FcεRI aggregation. Dynamic studies of MC activated by FcεRI aggregation have shown the migration of CD63-positive granules towards the plasma membrane (PM) followed by their fusion with the PM (17). As mentioned, we did not observe any decrease of total β-hexosaminidase levels in CD63−/− BMMC, making a storage defect unlikely. In addition, there were no ultrastructural difference in mast cell morphology and SL marker expression. This supports the hypothesis that CD63-deficiency specifically affects the release of mediators that are stored in SL, either directly or by inhibiting upstream signaling mechanisms.

The molecular details of distal events of MC degranulation such as membrane fusion, and their connection with FcεRI signaling, are now beginning to be understood. These processes are regulated by SNAREs (soluble N-ethyl-maleimide-sensitive factor-attachment protein receptors) (5, 7). The major t-SNARES (located on the target membrane) in MC degranulation appear to be syntaxin 4 and SNAP-23 (40–43), and the major v-SNARE appears to be VAMP-8 (42, 44–46). It remains to be elucidated how CD63 interfaces with this machinery. Given that PMA/ionomycin-induced degranulation, which circumvents FcεRI-induced signaling events that lead to activation of membrane fusion, is unaffected in CD63−/− BMMC, CD63 may be required for signaling events that feed into membrane fusion processes. Very proximal events such as FcεRI-induced global tyrosine phosphorylation and Akt phosphorylation (the latter was affected with anti-CD63 in RBL), were not affected in CD63-deficient BMMC. However, given the different cellular systems used and the different types of CD63 alterations (binding of surface-expressed CD63 by an antibody in the prior study, versus removal of both surface-expressed and intracellular granule-expressed CD63 by genetic targeting in the current study), differences in affected signaling pathways are to be expected. Regardless, the data obtained with both approaches

support an important role for CD63 in the degranulation process and allergic reactions *in vivo*.

A major signaling event during FcεRI-induced degranulation appears to be the activation of the t-SNARE SNAP23 through IKK2 (IKKβ) (43). Interestingly, IKK2-deficient BMMC not only show a defect in degranulation, but also in TNF-α secretion, similar to our observation in CD63-deficient BMMC in this study. In addition, IKK2 is a signaling molecule downstream of Akt, whose activation was suppressed by anti-CD63 in our previous study (16). Another recently described role for CD63 is recruitment of the calcium sensor synaptotagmin VII to lysosomes, which may provide another possible link between FcεRI signaling and CD63 (47). Further studies will focus on the role of CD63 in the mechanisms that regulate degranulation.

In our prior study using an anti-CD63 mAb and the RBL cell line, we observed that anti-CD63 inhibited degranulation only when tested on adherent cells (16). Anti-CD63 also inhibited RBL cell adhesion to extracellular matrix proteins. In our current study we used BMMC, which do not adhere spontaneously in contrast to RBL, which adhere very strongly to numerous surfaces. For example, in order to detach RBL cells from culture flasks incubation of several minutes at 37°C with trypsin and EDTA is required. CD63−/− BMMC showed diminished degranulation when triggered in suspension. Therefore, the requirement for adhesion to uncover the role of CD63 in RBL cells may be due to a particularity of these cells not shared by BMMC, or due to a CD63 antibody-induced effect that is not seen in cells genetically deficient for CD63. In addition, the prior study also suggested an inhibitory effect of anti-CD63 on the Gab2-PI3K–PKCδ pathway of degranulation (16). The possible mechanism of suppression in those studies included anti-CD63-mediated inhibition of adhesion signaling (which would then lead to diminished degranulation as a downstream effect), or alternatively, sequestering of signaling molecules required for both adhesion and degranulation. Given our new data in CD63−/− BMMC, the latter possibility appears more likely, given the robust inhibition of degranulation in suspended cells. While RBL cells have been used extensively as a model of MC, they may not be entirely representative of primary MC. For example, primary MC are heterogeneous depending on their degree of maturation, their tissue location, and whether they are resident or recruited to the site of an inflammatory reaction. They also differ in the presence of signaling molecules. For example, the tyrosine kinase Fyn, a regulator of FcεRI-induced degranulation in BMMC (48), is expressed at only very low levels in RBL cells. Therefore, differences should be expected depending on the source of MC used in the respective study.

The observed decrease in MC degranulation in CD63−/− BMMC and also with anti-CD63 in RBL cells (16) was approximately 50%. This strong, but partial inhibition may be due to the role of tetraspanins in multimeric complexes which incorporate other members of the tetraspanin family (12, 35), allowing for other tetraspanins to compensate for absent or inhibited CD63. This is also underscored by the observation that the defects in knockout models of other tetraspanins were generally mild (including the previously reported mild effects of CD63 in a knockout model) highlighting possible redundancies (25, 35). Candidate tetraspanins for cooperation with CD63 in mast cell degranulation are CD81, whose inhibition suppresses degranulation (15), and CD9, which is widely expressed on mast cells (13).

MC-mediated diseases such as allergic rhinoconjunctivitis or anaphylaxis, represent a significant health problem. Our observation of significantly impaired IgE-mediated allergic reactions both upon deletion of CD63 (as in this study) or with anti-CD63 antibodies (as in the prior studies), indicates that targeting CD63 for therapeutic purposes may represent a

promising avenue for therapy, and possibly for other inflammatory diseases in which MC have been implicated to play a pathogenic role.

Supplementary Material

Refer to Web version on PubMed Central for supplementary material.

REFERENCES

1. Hallgren J, Gurish MF. Mast cell progenitor trafficking and maturation. Adv Exp Med Biol. 2011; 716:14–28. [PubMed: 21713649]
2. Brown MA, Sayed BA, Christy A. Mast cells and the adaptive immune response. J Clin Immunol. 2008; 28:671–676. [PubMed: 18802742]
3. Galli SJ, Tsai M. Mast cells in allergy and infection: versatile effector and regulatory cells in innate and adaptive immunity. Eur J Immunol. 2010; 40:1843–1851. [PubMed: 20583030]
4. Beil WJ, Login GR, Aoki M, Lunardi LO, Morgan ES, Galli SJ, Dvorak AM. Tumor necrosis factor alpha immunoreactivity of rat peritoneal mast cell granules decreases during early secretion induced by compound 48/80: an ultrastructural immunogold morphometric analysis. Int Arch Allergy Immunol. 1996; 109:383–389. [PubMed: 8634524]
5. Benhamou M, Blank U. Stimulus-secretion coupling by high-affinity IgE receptor: new developments. FEBS Lett. 2010; 584:4941–4948. [PubMed: 20851120]
6. Gordon JR, Galli SJ. Mast cells as a source of both preformed and immunologically inducible TNF-alpha/cachectin. Nature. 1990; 346:274–276. [PubMed: 2374592]
7. Kalesnikoff J, Galli SJ. New developments in mast cell biology. Nat Immunol. 2008; 9:1215–1223. [PubMed: 18936782]
8. Kandere-Grzybowska K, Letourneau R, Kempuraj D, Donelan J, Poplawski S, Boucher W, Athanassiou A, Theoharides TC. IL-1 induces vesicular secretion of IL-6 without degranulation from human mast cells. J Immunol. 2003; 171:4830–4836. [PubMed: 14568962]
9. MacGlashan D Jr. IgE receptor and signal transduction in mast cells and basophils. Curr Opin Immunol. 2008; 20:717–723. [PubMed: 18822373]
10. Rivera J, Olivera A. A current understanding of Fc epsilon RI-dependent mast cell activation. Curr Allergy Asthma Rep. 2008; 8:14–20. [PubMed: 18377769]
11. Kraft S, Kinet JP. New developments in FcepsilonRI regulation, function and inhibition. Nat Rev Immunol. 2007; 7:365–378. [PubMed: 17438574]
12. Hemler ME. Tetraspanin functions and associated microdomains. Nat Rev Mol Cell Biol. 2005; 6:801–811. [PubMed: 16314869]
13. Koberle M, Kaesler S, Kempf W, Wolbing F, Biedermann T. Tetraspanins in Mast Cells. Front Immunol. 2012; 3:106. [PubMed: 22783251]
14. Yanez-Mo M, Barreiro O, Gordon-Alonso M, Sala-Valdes M, Sanchez-Madrid F. Tetraspanin-enriched microdomains: a functional unit in cell plasma membranes. Trends Cell Biol. 2009; 19:434–446. [PubMed: 19709882]
15. Fleming TJ, Donnadieu E, Song CH, Laethem FV, Galli SJ, Kinet JP. Negative regulation of Fc epsilon RI-mediated degranulation by CD81. J Exp Med. 1997; 186:1307–1314. [PubMed: 9334370]
16. Kraft S, Fleming T, Billingsley JM, Lin SY, Jouvin MH, Storz P, Kinet JP. Anti-CD63 antibodies suppress IgE-dependent allergic reactions in vitro and in vivo. J Exp Med. 2005; 201:385–396. [PubMed: 15684326]
17. Amano T, Furuno T, Hirashima N, Ohyama N, Nakanishi M. Dynamics of intracellular granules with CD63-GFP in rat basophilic leukemia cells. J Biochem. 2001; 129:739–744. [PubMed: 11328596]
18. Blott EJ, Griffiths GM. Secretory lysosomes. Nat Rev Mol Cell Biol. 2002; 3:122–131. [PubMed: 11836514]
19. Dragonetti A, Baldassarre M, Castino R, Demoz M, Luini A, Buccione R, Isidoro C. The lysosomal protease cathepsin D is efficiently sorted to and secreted from regulated secretory

compartments in the rat basophilic/mast cell line RBL. J Cell Sci. 2000; 113(Pt 18):3289–3298. [PubMed: 10954426]

20. Vincent-Schneider H, Thery C, Mazzeo D, Tenza D, Raposo G, Bonnerot C. Secretory granules of mast cells accumulate mature and immature MHC class II molecules. J Cell Sci. 2001; 114:323–334. [PubMed: 11148134]
21. Knol EF, Mul FP, Jansen H, Calafat J, Roos D. Monitoring human basophil activation via CD63 monoclonal antibody 435. J Allergy Clin Immunol. 1991; 88:328–338. [PubMed: 1716273]
22. Schafer T, Starkl P, Allard C, Wolf RM, Schweighoffer T. A granular variant of CD63 is a regulator of repeated human mast cell degranulation. Allergy. 2010; 65:1242–1255. [PubMed: 20337613]
23. Kitani S, Berenstein E, Mergenhagen S, Tempst P, Siraganian RP. A cell surface glycoprotein of rat basophilic leukemia cells close to the high affinity IgE receptor (Fc epsilon RI). Similarity to human melanoma differentiation antigen ME491. J Biol Chem. 1991; 266:1903–1909. [PubMed: 1703158]
24. Nishikata H, Oliver C, Mergenhagen SE, Siraganian RP. The rat mast cell antigen AD1 (homologue to human CD63 or melanoma antigen ME491) is expressed in other cells in culture. J Immunol. 1992; 149:862–870. [PubMed: 1634775]
25. Schroder J, Lullmann-Rauch R, Himmerkus N, Pleines I, Nieswandt B, Orinska Z, Koch-Nolte F, Schroder B, Bleich M, Saftig P. Deficiency of the tetraspanin CD63 associated with kidney pathology but normal lysosomal function. Mol Cell Biol. 2009; 29:1083–1094. [PubMed: 19075008]
26. van Niel G, Charrin S, Simoes S, Romao M, Rochin L, Saftig P, Marks MS, Rubinstein E, Raposo G. The tetraspanin CD63 regulates ESCRT-independent and -dependent endosomal sorting during melanogenesis. Dev Cell. 2011; 118:4265–4273.
27. Doyle EL, Ridger V, Ferraro F, Turmaine M, Saftig P, Cutler DF. CD63 is an essential cofactor to leukocyte recruitment by endothelial P-selectin. Blood. 2011; 118:4265–4273. [PubMed: 21803846]
28. Dvorak AM. Procedural guide to specimen handling for the ultrastructural pathology service laboratory. Journal of Electron Microscopy Technique. 1987; 6:255–301.
29. Savalas LR, Gasnier B, Damme M, Lubke T, Wrocklage C, Debacker C, Jezegou A, Reinheckel T, Hasilik A, Saftig P, Schroder B. Disrupted in renal carcinoma 2 (DIRC2), a novel transporter of the lysosomal membrane, is proteolytically processed by cathepsin L. Biochem J. 2011; 439:113–128. [PubMed: 21692750]
30. Pohlmann R, Boeker MW, von Figura K. The two mannose 6-phosphate receptors transport distinct complements of lysosomal proteins. J Biol Chem. 1995; 270:27311–27318. [PubMed: 7592993]
31. Zachos C, Blanz J, Saftig P, Schwake M. A critical histidine residue within LIMP-2 mediates pH sensitive binding to its ligand beta-glucocerebrosidase. Traffic. 2012; 13:1113–1123. [PubMed: 22537104]
32. Rivera J, Kinet JP, Kim J, Pucillo C, Metzger H. Studies with a monoclonal antibody to the beta subunit of the receptor with high affinity for immunoglobulin E. Mol Immunol. 1988; 25:647–661. [PubMed: 2971137]
33. Storz P, Toker A. Protein kinase D mediates a stress-induced NF-kappaB activation and survival pathway. EMBO J. 2003; 22:109–120. [PubMed: 12505989]
34. Tsai M, Wedemeyer J, Ganiatsas S, Tam SY, Zon LI, Galli SJ. In vivo immunological function of mast cells derived from embryonic stem cells: an approach for the rapid analysis of even embryonic lethal mutations in adult mice in vivo. Proc Natl Acad Sci U S A. 2000; 97:9186–9190. [PubMed: 10908668]
35. Hemler ME. Targeting of tetraspanin proteins--potential benefits and strategies. Nat Rev Drug Discov. 2008; 7:747–758. [PubMed: 18758472]
36. Griffiths G. What's special about secretory lysosomes? Semin Cell Dev Biol. 2002; 13:279–284. [PubMed: 12243727]

37. Bonifacino JS, Perez P, Klausner RD, Sandoval IV. Study of the transit of an integral membrane protein from secretory granules through the plasma membrane of secreting rat basophilic leukemia cells using a specific monoclonal antibody. J Cell Biol. 1986; 102:516–522. [PubMed: 3511074]
38. Raposo G, Tenza D, Mecheri S, Peronet R, Bonnerot C, Desaymard C. Accumulation of major histocompatibility complex class II molecules in mast cell secretory granules and their release upon degranulation. Mol Biol Cell. 1997; 8:2631–2645. [PubMed: 9398681]
39. Schwartz LB, Austen KF. Enzymes of the mast cell granule. J Invest Dermatol. 1980; 74:349–353. [PubMed: 6771334]
40. Guo Z, Turner C, Castle D. Relocation of the t-SNARE SNAP-23 from lamellipodia-like cell surface projections regulates compound exocytosis in mast cells. Cell. 1998; 94:537–548. [PubMed: 9727496]
41. Hepp R, Puri N, Hohenstein AC, Crawford GL, Whiteheart SW, Roche PA. Phosphorylation of SNAP-23 regulates exocytosis from mast cells. J Biol Chem. 2005; 280:6610–6620. [PubMed: 15611044]
42. Paumet F, Le Mao J, Martin S, Galli T, David B, Blank U, Roa M. Soluble NSF attachment protein receptors (SNAREs) in RBL-2H3 mast cells: functional role of syntaxin 4 in exocytosis and identification of a vesicle-associated membrane protein 8-containing secretory compartment. J Immunol. 2000; 164:5850–5857. [PubMed: 10820264]
43. Suzuki K, Verma IM. Phosphorylation of SNAP-23 by IkappaB kinase 2 regulates mast cell degranulation. Cell. 2008; 134:485–495. [PubMed: 18692471]
44. Puri N, Roche PA. Mast cells possess distinct secretory granule subsets whose exocytosis is regulated by different SNARE isoforms. Proc Natl Acad Sci U S A. 2008; 105:2580–2585. [PubMed: 18250339]
45. Sander LE, Frank SP, Bolat S, Blank U, Galli T, Bigalke H, Bischoff SC, Lorentz A. Vesicle associated membrane protein (VAMP)-7 and VAMP-8, but not VAMP-2 or VAMP-3, are required for activation-induced degranulation of mature human mast cells. Eur J Immunol. 2008; 38:855–863. [PubMed: 18253931]
46. Tiwari N, Wang CC, Brochetta C, Ke G, Vita F, Qi Z, Rivera J, Soranzo MR, Zabucchi G, Hong W, Blank U. VAMP-8 segregates mast cell-preformed mediator exocytosis from cytokine trafficking pathways. Blood. 2008; 111:3665–3674. [PubMed: 18203950]
47. Flannery AR, Czibener C, Andrews NW. Palmitoylation-dependent association with CD63 targets the Ca2+ sensor synaptotagmin VII to lysosomes. J Cell Biol. 2010; 191:599–613. [PubMed: 21041449]
48. Parravicini V, Gadina M, Kovarova M, Odom S, Gonzalez-Espinosa C, Furumoto Y, Saitoh S, Samelson LE, O'Shea JJ, Rivera J. Fyn kinase initiates complementary signals required for IgE-dependent mast cell degranulation. Nat Immunol. 2002; 3:741–748. [PubMed: 12089510]

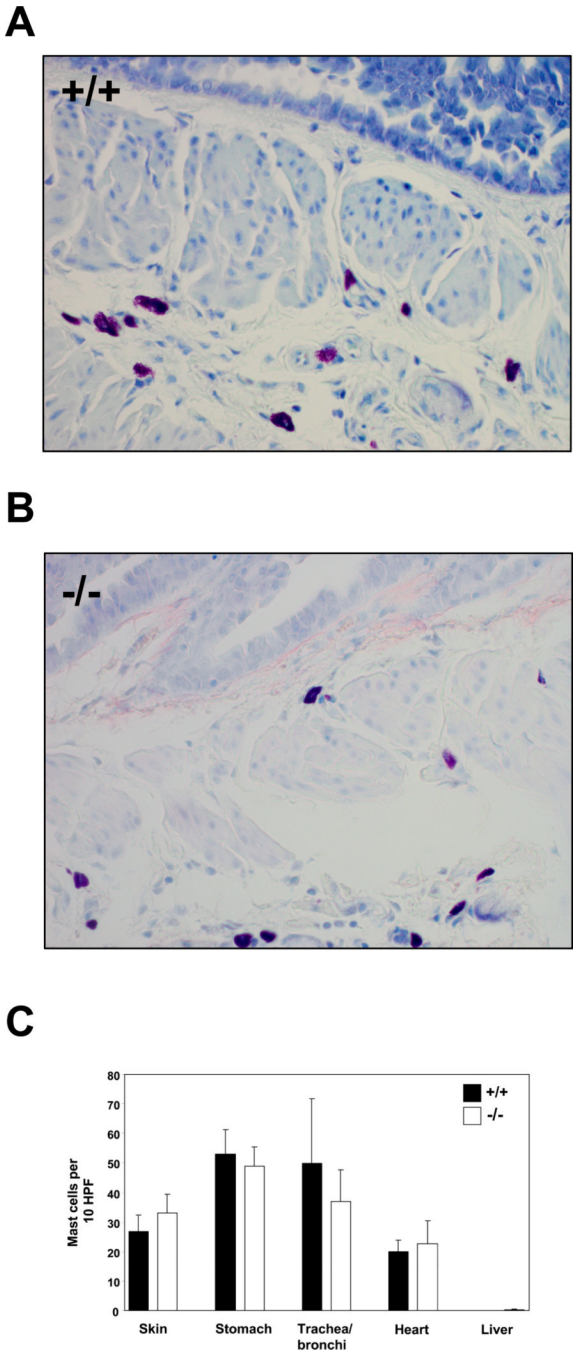

Figure 1. CD63 −/− mice show normal numbers and tissue distribution of mast cells (MC)
Staining of MC in bronchial walls of (A) CD63 +/+ and (B) CD63 −/− mice by toluidine blue. (C) Tissue MC numbers in skin, stomach, trachea/bronchi and heart of CD63 +/+ and CD63 −/− littermates (mean +/− standard deviation; 3 mice per genotype; 10 HPF counted twice per condition).

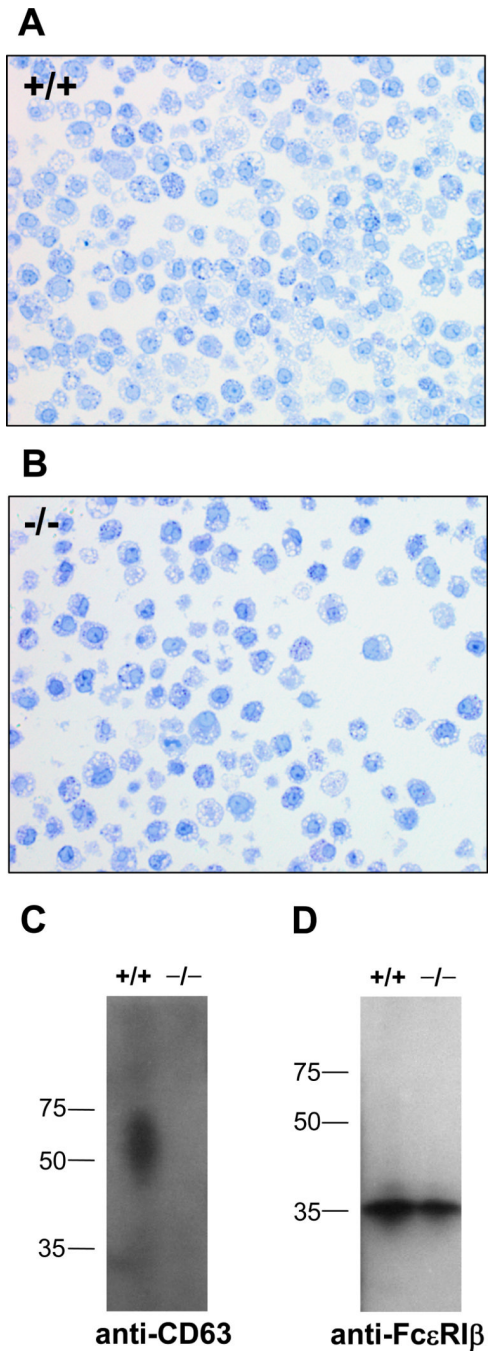

Figure 2. Bone marrow-derived mast cells (BMMC) from CD63 −/− mice show no overt morphological differences to BMMC from CD63 +/+ mice and lack CD63 protein expression

Giemsa-stained preparations from CD63 +/+ BMMC (A) and CD63 −/− BMMC (B). Lysates from CD63 +/+ and CD63 −/− BMMC were blotted with anti-CD63 (C) or anti-FcεRIβ as a control (D).

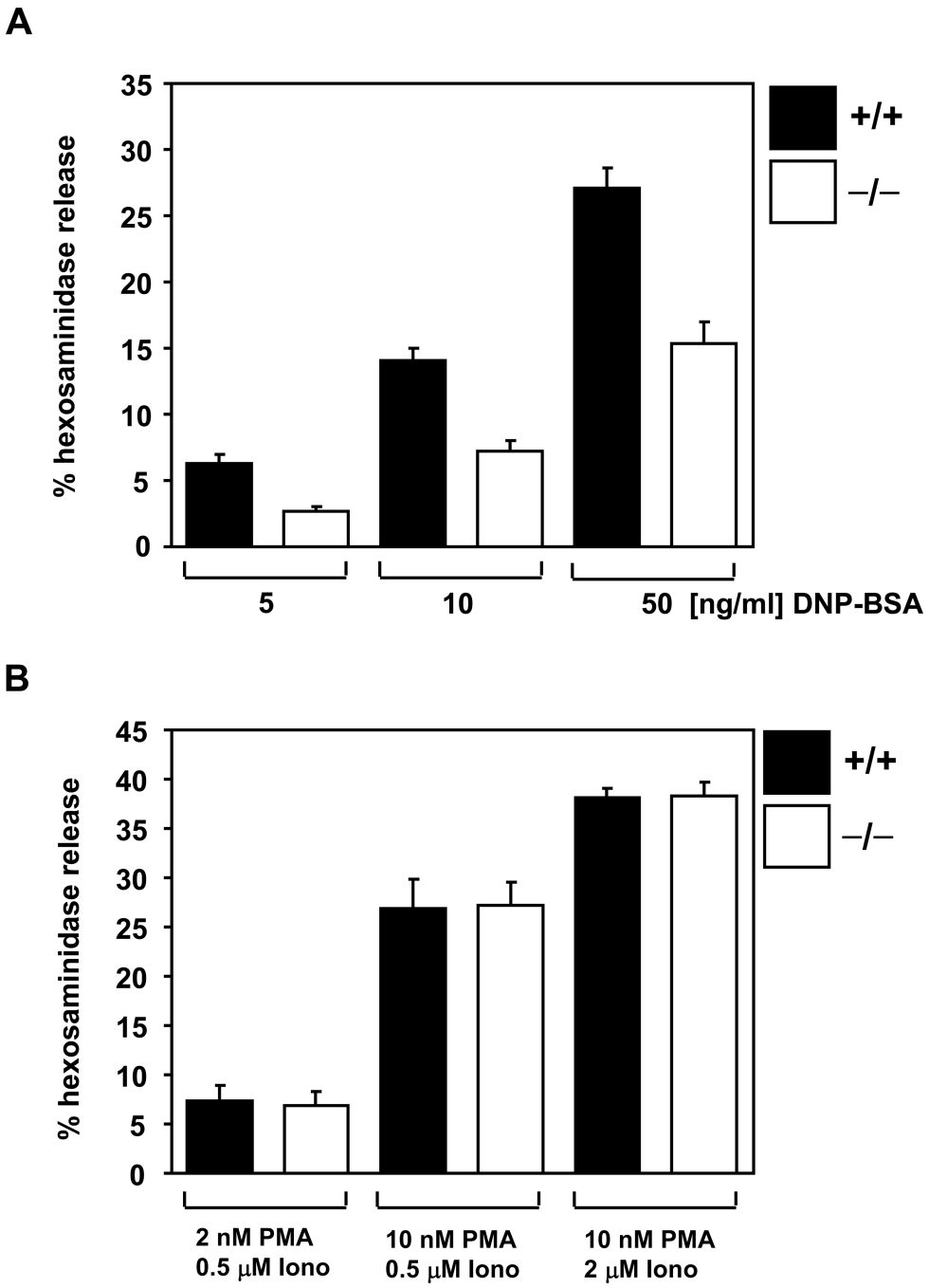

Figure 3. CD63 −/− BMMC show diminished FcεRI aggregation-induced degranulation and similar PMA/ionomycin-induced degranulation

CD63+/+ and CD63−/− BMMCs were loaded with anti-DNP IgE and (A) triggered with DNP BSA for FcεRI-induced activation or (B) a combination of PMA and ionomycin for 30 minutes. Supernatants were assayed for β-hexosaminidase with the substrate p-nitrophenyl N-acetyl-β-D-glucosaminide. Results are expressed as mean + SEM of release calculated as % of total β-hexosaminidase content and after subtraction of baseline degranulation in untriggered cells (n=10 for CD63+/+ and n=9 for CD63−/− BMMC cultures from littermates in 3 independent experiments with $p < 0.0001$ for (A); n=6 each for CD63+/+ and CD63−/− BMMC cultures from littermates in 4 independent experiments with p =

0.8298, p = 0.9597, and p = 0.9892 for 2 nM/0.5 μM, 10 nM/0.5 μM, and 10 nM/ 2μM PMA/ionomycin respectively for (B)).

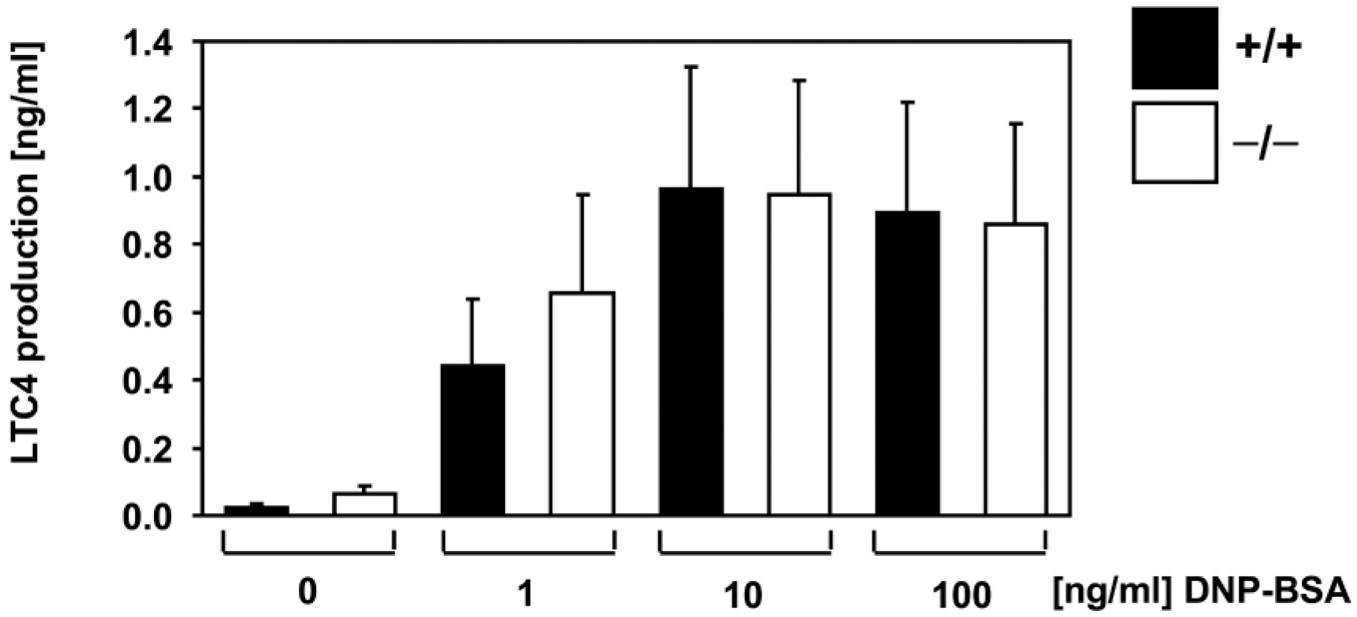

Figure 4. FcεRI aggregation-induced leukotriene C4 (LTC4) production is not significantly different in CD63+/+ and CD63−/− BMMC

CD63+/+ and CD63−/− BMMCs were loaded with anti-DNP IgE and triggered with DNP BSA (0–100 ng/ml) for 30 minutes. LTC4 was measured in the supernatants by EIA. Results are expressed as mean + SEM from 3 independent experiments performed each with BMMC from one CD63+/+ and one CD63−/− littermate).

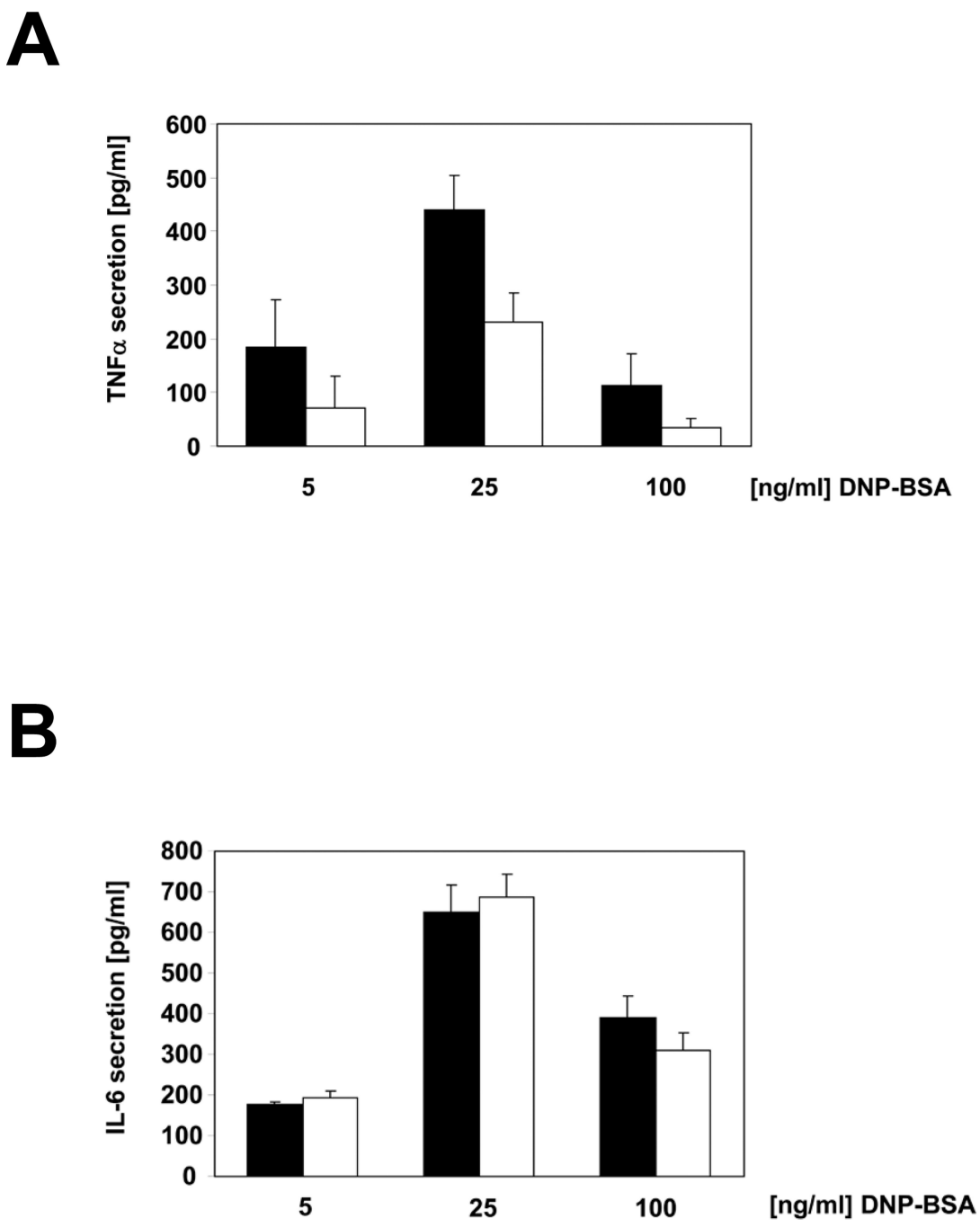

Figure 5. FcεRI aggregation-induced TNFα secretion, but not IL-6 secretion, is reduced in CD63−/− BMMC

CD63+/+ and CD63−/− BMMCs were loaded with anti-DNP IgE and triggered with DNP HSA (0–100 ng/mL) for 6 hours. Supernatants were assayed for TNFα (A) and IL-6 (B) by ELISA against a standard curve. TNFα: mean +/− SEM after subtraction of background (one experiment representative of three independent experiments performed each with one CD63+/+ mouse and one CD63−/− littermate). IL-6: one experiment representative of two independent experiments performed each with one CD63+/+ mouse and one CD63−/− littermate.

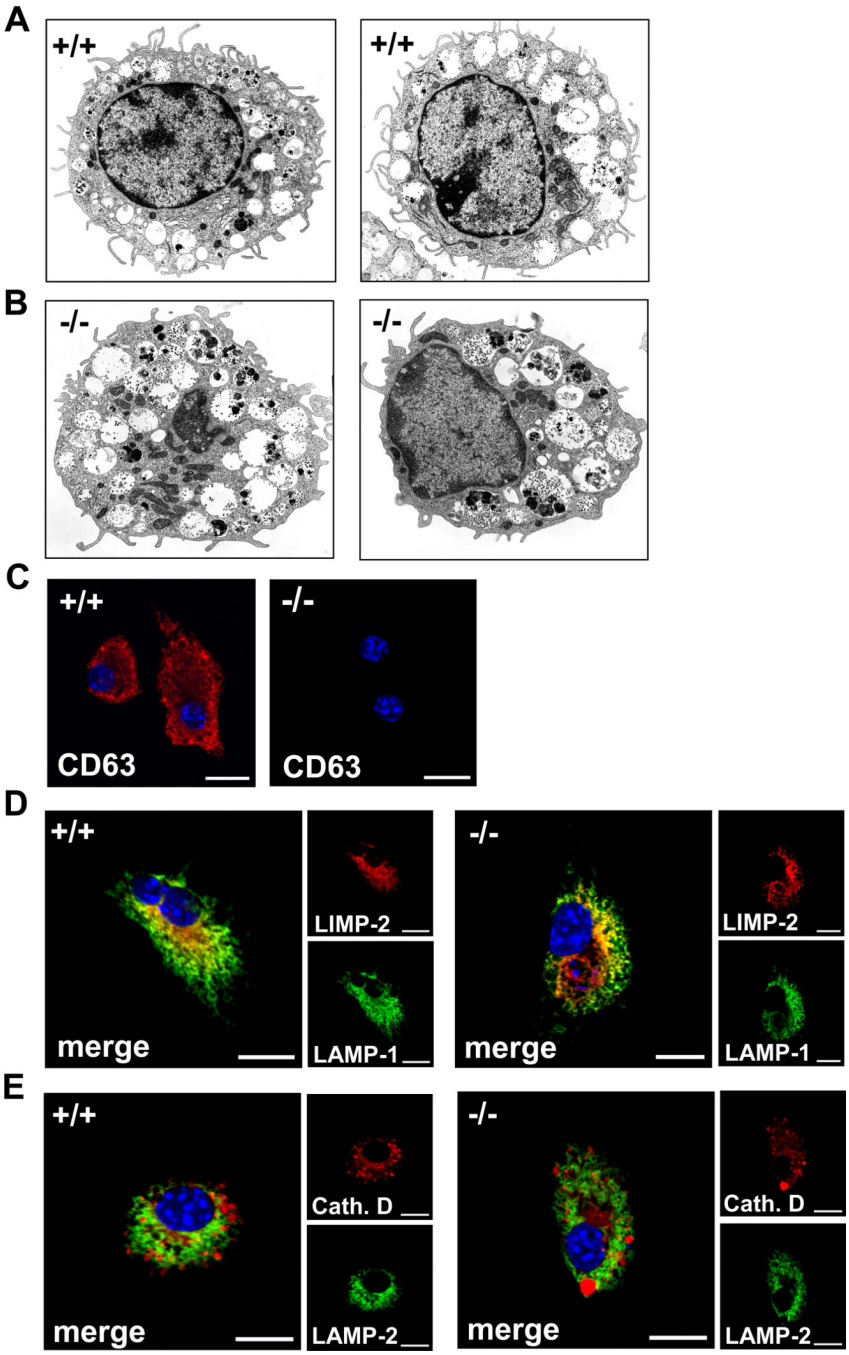

Figure 6. CD63+/+ and CD63−/− BMMC do not show discernible ultrastructural differences and late endosomal/lysosomal marker expression

Electron microcopy of CD63+/+ (A) and CD63−/− (B) BMMC shows immature mast cells with a large nucleus with partially dispersed chromatin, narrow surface folds, and many membrane-bound cytoplasmic secretory granules which are only partially filled with a mixture of membranous and dense materials (data shown are representative for two independent experiments, performed in two different facilities (Boston, MA, and Kiel, Germany). Indirect immunofluorescence and confocal microscopy shows absence of CD63 expression in CD63−/− BMMC (C), but comparable expression and distribution of late endosomal/lysosomal proteins LIMP-2 and LAMP-1 (D), as well as cathepsin D and

LAMP-2 (E). Scale bars: 10 μm. Data shown are representative of two independent experiments.

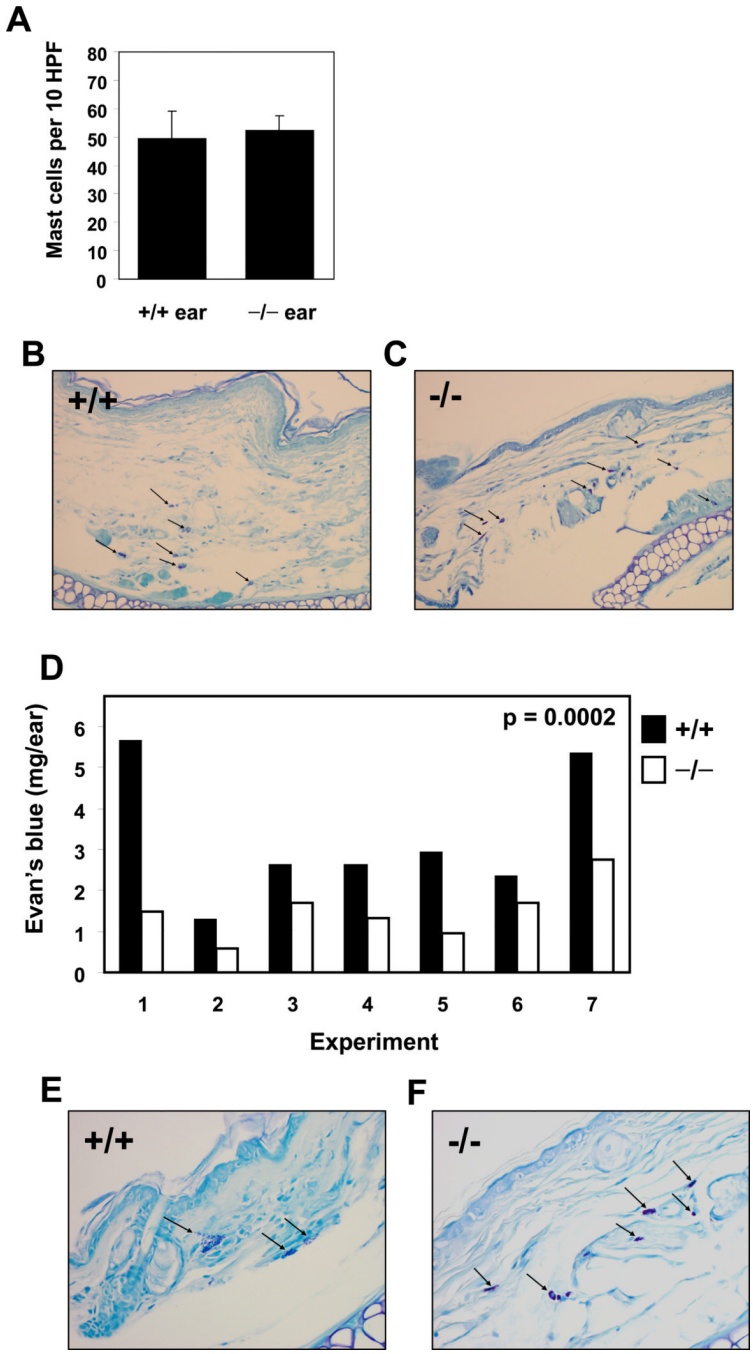

Figure 7. IgE-mediated passive cutaneous anaphylaxis in ears of MC reconstituted Kit$^{W/W\text{-}V}$ mice is reduced in ears reconstituted with CD63−/− BMMC compared to ears reconstituted with CD63+/+ BMMC

Kit$^{W/W\text{-}V}$ mice were reconstituted by intradermal injection in 1 ear with 1×10^6 CD63+/+ BMMC and with the same number of CD63−/− BMMC in the other ear. (A) MC numbers were counted per 10 HPF on toluidine blue stains. Mean +/− SEM from two independent experiments. (B, C) Toluidine blue stains of sections from ears after WT or CD63−/− BMMC reconstitution. (D) Extravasated Evan's blue was extracted from ears after PCA and measured. Three independent experiments performed with BMMC from a total of 7 CD63+/+ mice and 7 CD63−/− littermates. (E, F) In a separate similar experiment performed

without Evan's blue the ears were harvested and stained with toluidine blue to assess degranulation in the CD63+/+ BMMC reconstituted ear (E) and in the CD63−/− BMMC reconstituted ear (F).